IMPROVED ROBUSTNESS OF MULTIVARIABLE MODEL PREDICTIVE CONTROL UNDER MODEL UNCERTAINTIES

Cristina Stoica, Pedro Rodríguez-Ayerbe and Didier Dumur
Department of Automatic Control, Supélec, 3 rue Joliot Curie, F91192 Gif-sur-Yvette, France
cristina.stoica@supelec.fr, pedro.rodriguez@supelec.fr, didier.dumur@supelec.fr

Keywords: Model Predictive Control (MPC), Multivariable Systems, Linear Matrix Inequalities, Robust Control.

Abstract: This paper presents a state-space methodology for enhancing the robustness of multivariable MPC controlled systems through the convex optimization of a multivariable Youla parameter. The procedure starts with the design of an initial stabilizing Model Predictive Controller in the state-space representation, which is then robustified under modeling errors considered as unstructured uncertainties. The resulting robustified MIMO control law is finally applied to the model of a stirred tank reactor to reduce the impact of measurement noise and modelling errors on the system.

1 INTRODUCTION

Model predictive control strategies are widely used in industrial applications, resulting in improved performance, with a practical implementation of the controller which remains simple. However, starting with a controller design based on a 'nominal' model of the system, the question of its robustness towards model uncertainties or disturbances acting on the system always occurs in an industrial environment.

Some methods in the literature deal with robustness maximisation, but in the transfer function formalism (Kouvaritakis et al., 1992), (Yoon and Clarke, 1995), (Dumur and Boucher, 1998), and mainly applied to SISO systems, which makes the generalization to multivariable systems much more complicated.

The purpose of this paper is to present a methodology enhancing the robustness of an initial MIMO predictive controller towards model uncertainties. The state-space design allows the robustification process to be handled in a convenient way. A two-step procedure is followed. An initial MIMO MPC controller is first designed, its robustness is then enhanced via the Youla parametrization, without significantly increasing the complexity of the final control law. The Youla parametrization allows formulating frequency constraints as convex optimization, the entire problem being solved with LMI (Linear Matrix Inequality) techniques.

The paper is organized as follows. Section 2 reminds the main steps leading to the MPC controller in the state-space representation. Section 3 gives the background material required to formulate the robustification strategy, from the Youla parametrization to the robustness criteria under unstructured uncertainties. The elaboration of the robustified controller in state-space representation for this type of uncertainties is further proposed in Section 4. Section 5 provides the application of this control strategy to a stirred tank reactor. Section 6 presents some conclusions and further perspectives.

2 MIMO MPC IN STATE-SPACE FORMULATION

This section focuses on the design of an initial MIMO MPC law. Compared to approaches proposed in the literature based on transfer function formalism, the state-space representation framework chosen here (Camacho and Bordons, 2004) leads to a simplified formulation and reduced computation efforts for MIMO systems. Consider the following discrete time MIMO LTI system:

$$\begin{cases} \mathbf{x}(k+1) = \mathbf{A}\,\mathbf{x}(k) + \mathbf{B}\mathbf{u}(k) \\ \mathbf{y}(k) = \mathbf{C}\,\mathbf{x}(k) \end{cases} \tag{1}$$

where $\mathbf{A} \in \mathbf{R}^{n\times n}$, $\mathbf{B} \in \mathbf{R}^{n\times m}$, $\mathbf{C} \in \mathbf{R}^{p\times n}$ are the system state-space matrices, $\mathbf{x} \in \mathbf{R}^{n\times 1}$ describes the MIMO system states, $\mathbf{u} \in \mathbf{R}^{m\times 1}$ is the input vector and $\mathbf{y} \in \mathbf{R}^{p\times 1}$ is the output vector.

Next step is to add an integral action to this state-space representation which will guarantee cancellation of steady-state errors:

$$\mathbf{u}(k) = \mathbf{u}(k-1) + \Delta\mathbf{u}(k) \tag{2}$$

This results in an increase of the system states as:

$$\begin{cases}\mathbf{x}_e(k+1) = \mathbf{A}_e\,\mathbf{x}_e(k) + \mathbf{B}_e\,\Delta\mathbf{u}(k) \\ \mathbf{y}(k) = \mathbf{C}_e\,\mathbf{x}_e(k)\end{cases} \tag{3}$$

where the extended state-space representation $\mathbf{x}_e(k) = \left[\mathbf{x}^T(k)\ \ \mathbf{u}^T(k-1)\right]^T$ is characterized by:

$$\mathbf{A}_e = \begin{bmatrix}\mathbf{A} & \mathbf{B}\\ \mathbf{0}_{m,n} & \mathbf{I}_m\end{bmatrix},\ \mathbf{B}_e = \begin{bmatrix}\mathbf{B}\\ \mathbf{I}_m\end{bmatrix},\ \mathbf{C}_e = \left[\mathbf{C}\ \ \mathbf{0}_{p,m}\right].$$

The control signal is derived by minimizing the following quadratic objective function:

$$J = \sum_{i=N_1}^{N_2}\left\|\hat{\mathbf{y}}(k+i) - \mathbf{w}(k+i)\right\|^2_{\tilde{\mathbf{Q}}_J(i)} + \sum_{i=0}^{N_u-1}\left\|\Delta\mathbf{u}(k+i)\right\|^2_{\tilde{\mathbf{R}}_J(i)} \tag{4}$$

where the future control increments $\Delta\mathbf{u}(k+i)$ are supposed to be zero for $i \ge N_u$. The signal $\mathbf{w}$ represents the setpoint. It is assumed in further developments that the same output prediction horizons (N_1, N_2) and the same control horizon N_u is applied for all input/output transfer functions. $\tilde{\mathbf{Q}}_J$ and $\tilde{\mathbf{R}}_J$ are weighting matrices. The predicted output vector has the following form:

$$\hat{\mathbf{y}}(k+i) = \mathbf{C}\,\mathbf{A}^i\hat{\mathbf{x}}(k) + \sum_{j=0}^{i-1}\mathbf{C}\,\mathbf{A}^{i-j-1}\mathbf{B}\mathbf{u}(k+j) \tag{5}$$

where the input vector can be written as:

$$\mathbf{u}(k+j) = \mathbf{u}(k-1) + \sum_{l=0}^{j}\Delta\mathbf{u}(k+l) \tag{6}$$

The state estimate is derived from the observer:

$$\hat{\mathbf{x}}_e(k+1) = \mathbf{A}_e\,\hat{\mathbf{x}}_e(k) + \mathbf{B}_e\,\Delta\mathbf{u}(k) + \mathbf{K}[\mathbf{y}(k) - \mathbf{C}_e\,\hat{\mathbf{x}}_e(k)] \tag{7}$$

The multivariable observer gain $\mathbf{K}$ is designed through a classical method of eigenvectors, arbitrarily placing the eigenvalues of $\mathbf{A}_e - \mathbf{K}\mathbf{C}_e$ in a stable region, as detailed in (Magni, 2002). The observer gain $\mathbf{K}$ is obtained from the extended state-space description and will be used for further mathematical calculation in the robustification procedure. However this design aspect is not crucial since the convex robustification method should lead to an optimal set of these eigenvalues. Moreover the input/output transfer function is not influenced by the eigenvalues placement used to find $\mathbf{K}$ (Boyd and Barratt, 1991).

The objective function can be rewritten in the matrix formalism (Maciejowski, 2001):

$$J = \left\|\mathbf{Y}(k) - \mathbf{W}(k)\right\|^2_{\mathbf{Q}_J} + \left\|\Delta\mathbf{U}(k)\right\|^2_{\mathbf{R}_J} \tag{8}$$

where $\mathbf{Q}_J = diag(\tilde{\mathbf{Q}}_J(N_1), \cdots, \tilde{\mathbf{Q}}_J(N_2))$,

$\mathbf{R}_J = diag(\tilde{\mathbf{R}}_J(0), \cdots, \tilde{\mathbf{R}}_J(N_u - 1))$,

$\mathbf{Y}(k) = \left[\hat{\mathbf{y}}^T(k+N_1)\ \cdots\ \hat{\mathbf{y}}^T(k+N_2)\right]^T$,

$\mathbf{W}(k) = \left[\mathbf{w}^T(k+N_1)\ \cdots\ \mathbf{w}^T(k+N_2)\right]^T$,

$\Delta\mathbf{U}(k) = \left[\Delta\mathbf{u}^T(k)\ \cdots\ \Delta\mathbf{u}^T(k+N_u-1)\right]^T$.

Using these notations, the output vector $\mathbf{Y}(k)$ can be written in the following matrix form, with the definition of the vector $\mathbf{\Theta}(k)$ as a tracking error:

$$\mathbf{Y}(k) = \mathbf{\Psi}\,\hat{\mathbf{x}}(k) + \mathbf{\Phi}\,\mathbf{u}(k-1) + \mathbf{\Phi}_\Delta\Delta\mathbf{U}(k) \tag{9}$$

$$\mathbf{\Theta}(k) = \mathbf{W}(k) - \mathbf{\Psi}\,\hat{\mathbf{x}}(k) - \mathbf{\Phi}\,\mathbf{u}(k-1) \tag{10}$$

with $\mathbf{\Psi} = \left[(\mathbf{C}\mathbf{A}^{N_1})^T\ \cdots\ (\mathbf{C}\mathbf{A}^{N_2})^T\right]^T$,

$\mathbf{\Phi} = \left[\mathbf{\Sigma}^T_{N_1-1}\ \cdots\ \mathbf{\Sigma}^T_{N_2-1}\right]^T$, $\mathbf{\Sigma}_i = \mathbf{C}\sum_{j=0}^{i}\mathbf{A}^{i-j}\mathbf{B}$, $\mathbf{\Sigma}^T_i = (\mathbf{\Sigma}_i)^T$,

$$\mathbf{\Phi}_\Delta = \begin{bmatrix}\mathbf{\Sigma}_{N_1-1} & \cdots & \mathbf{\Sigma}_0 & 0 & \cdots & 0\\ \vdots & \cdots & \vdots & \vdots & \ddots & \vdots\\ \mathbf{\Sigma}_{N_2-1} & \cdots & \mathbf{\Sigma}_{N_2-N_1} & \mathbf{\Sigma}_{N_2-N_1-1} & \cdots & \mathbf{\Sigma}_{N_2-N_u}\end{bmatrix}.$$

The objective function is now given by:

$$J = \left\|\mathbf{\Phi}_\Delta\Delta\mathbf{U}(k) - \mathbf{\Theta}(k)\right\|^2_{\mathbf{Q}_J} + \left\|\Delta\mathbf{U}(k)\right\|^2_{\mathbf{R}_J} \tag{11}$$

which analytical minimization provides:

$$\Delta\mathbf{U}(k) = (\mathbf{R}_J + \mathbf{\Phi}^{\mathrm{T}}_\Delta\mathbf{Q}_J\mathbf{\Phi}_\Delta)^{-1}\mathbf{\Phi}^{\mathrm{T}}_\Delta\,\mathbf{Q}_J\,\mathbf{\Theta}(k) \tag{12}$$

Applying the receding horizon principle, only the first component of each future control sequence is applied to the system, meaning that the first m lines of $\Delta\mathbf{U}(k)$ are used:

$$\Delta\mathbf{u}(k) = \boldsymbol{\mu}\,\mathbf{\Theta}(k) \tag{13}$$

with $\boldsymbol{\mu} = \left[\mathbf{I}_m\ \ \mathbf{0}_{m,m(N_u-1)}\right](\mathbf{R}_J + \mathbf{\Phi}^{\mathrm{T}}_\Delta\,\mathbf{Q}_J\,\mathbf{\Phi}_\Delta)^{-1}\mathbf{\Phi}^{\mathrm{T}}_\Delta\,\mathbf{Q}_J$.

The system model, the observer and the predictive control can be represented in the state-space formulation according to Figure 1. The control signal depends on the control gain $\mathbf{L} = \left[\mathbf{L}_1\ \ \mathbf{L}_2\right]$ and the setpoint filter $\mathbf{F}_w$:

$$\Delta\mathbf{u}(k) = \mathbf{F}_w\mathbf{w}(k) - \mathbf{L}\,\hat{\mathbf{x}}_e(k) \tag{14}$$

with $\mathbf{L}_1 = \boldsymbol{\mu}\mathbf{\Psi}$, $\mathbf{L}_2 = \boldsymbol{\mu}\mathbf{\Phi}$, $\mathbf{F}_w = diag(\mathbf{F}_{w,1}, \cdots, \mathbf{F}_{w,p})$ related to the structure of $\boldsymbol{\mu}$ and $\mathbf{w}(k)$.

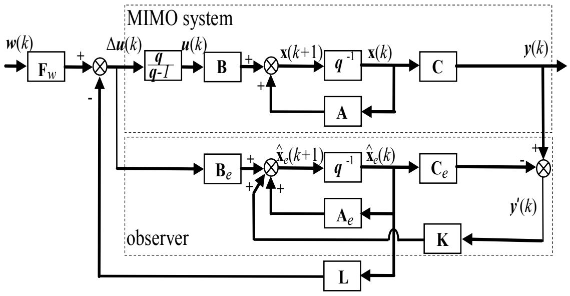

Figure 1: Block diagram of MIMO MPC.

3 ROBUSTNESS USING THE YOULA PARAMETER

This section overviews a technique that improves the robustness of the previous multivariable MPC law in terms of the Youla parameter, also named **Q** parameter. Any stabilizing controller (Boyd and Barratt, 1991), (Maciejowski, 1989) can be represented by a state-space feedback controller coupled with an observer and a Youla parameter. This part focuses on the main steps leading to the multivariable **Q** parameter (here with p inputs and m outputs) that robustifies the MPC law described in Section 2.

3.1 Stabilizing Control Law

The whole class of stabilizing control law can be obtained from an initial stabilizing controller via the Youla parametrization. The first step considers additional inputs $\mathbf{u}'$ and outputs $\mathbf{y}'$ with a zero transfer between them ($\mathbf{T}_{22} = 0$ in Figure 2).

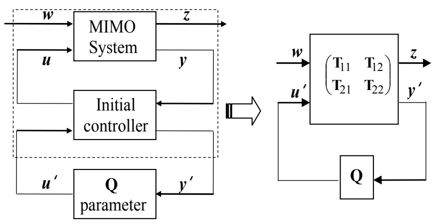

Figure 2: Class of all stabilizing multivariable controllers.

The Youla parameter is then added between $\mathbf{y}'$ and $\mathbf{u}'$ without restricting closed-loop stability. In this case, the transfer from $\mathbf{u}$ to $\mathbf{y}$ remains unchanged. As a result, the closed-loop function between $\mathbf{w}$ and $\mathbf{z}$ is linearly parametrized by the **Q** parameter, allowing convex specification (Boyd and Barratt, 1991):

$$\mathbf{T_{zw}} = \mathbf{T}_{11\,\mathbf{zw}} + \mathbf{T}_{12\,\mathbf{zw}}\,\mathbf{Q}\,\mathbf{T}_{21\,\mathbf{zw}} \tag{15}$$

where $\mathbf{T}_{11}, \mathbf{T}_{12}, \mathbf{T}_{21}$ depends on the input vector $\mathbf{w}$ and output vector $\mathbf{z}$ considered.

3.2 Robustness Under Frequency Constraints

Practical applications always deal with neglected dynamics and potential disturbances, so that robustness under unstructured uncertainties must be addressed as shown in Figure 3.

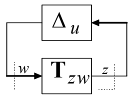

Figure 3: Unstructured uncertainty.

According to the small gain theorem (Maciejowski, 1989), robustness under unstructured uncertainties Δ_u is maximized as:

$$\min_{\mathbf{Q}\in\Re H_\infty} \left\| \mathbf{T_{zw}} \mathbf{W}_T \right\|_\infty \tag{16}$$

where the weighting term $\mathbf{W}_T$ reflects the frequency range where model uncertainties are more important. For multivariable systems, the H_∞ norm can be calculated as the maximum of the higher singular values. The following theorem formulates the previous H_∞ norm minimization.

Theorem (Clement and Duc, 2000) and (Boyd et al., 1994): A discrete time system given by the state-space representation $(\mathbf{A}_{cl}, \mathbf{B}_{cl}, \mathbf{C}_{cl}, \mathbf{D}_{cl})$ is stable and admits a H_∞ norm lower than γ if and only if:

$$\exists \mathbf{X}_1 = \mathbf{X}_1^{\mathrm{T}} > 0 \,/ \begin{bmatrix} -\mathbf{X}_1^{-1} & \mathbf{A}_{cl} & \mathbf{B}_{cl} & \mathbf{0} \\ \mathbf{A}_{cl}^{\mathrm{T}} & -\mathbf{X}_1 & \mathbf{0} & \mathbf{C}_{cl}^{\mathrm{T}} \\ \mathbf{B}_{cl}^{\mathrm{T}} & \mathbf{0} & -\gamma\mathbf{I} & \mathbf{D}_{cl}^{\mathrm{T}} \\ \mathbf{0} & \mathbf{C}_{cl} & \mathbf{D}_{cl} & -\gamma\mathbf{I} \end{bmatrix} < 0 \tag{17}$$

This expression can be transformed into a LMI, which variables are $\mathbf{X}_1$, γ and the **Q** parameter included in the closed-loop matrices, as shown in (Clement and Duc, 2000). As a result, the optimization problem is formulated as the minimization of γ under this LMI constraint.

4 ROBUSTIFIED MIMO MPC

The previous robustification strategy based on the Youla parameter is now applied to an initial MIMO state-space MPC calculated as shown in Section 2. The robustness maximization under additive unstructured uncertainties is also equivalent to the minimization of the influence of a measurement noise $\mathbf{b}$ on the control signal $\mathbf{u}$ (Figure 4); the transfer (15) between $\mathbf{w}$ and $\mathbf{z}$ corresponds to the transfer from $\mathbf{b}$ to $\mathbf{u}$. The H_∞ norm of this transfer will be further minimized using LMI tools.

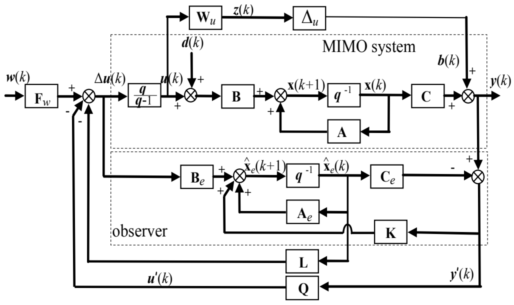

Figure 4: Stabilizing MIMO MPC via **Q** parametrization.

4.1 Stabilizing Control Law

Consider the MIMO linear discrete time system in the state-space representation, including an integral action (3). After adding an auxiliary input vector $\mathbf{u}'$ and output vector $\mathbf{y}'$ (Figure 4), the multivariable control signal is computed as described in Section 2:

$$\Delta\mathbf{u}(k) = \mathbf{F}_w\mathbf{w}(k) - \mathbf{L}\,\hat{\mathbf{x}}_e(k) - \mathbf{u}'(k) \tag{18}$$

with the following observer:

$$\begin{aligned}\hat{\mathbf{x}}_e(k+1) = \mathbf{A}_e\,\hat{\mathbf{x}}_e(k) + \mathbf{B}_e\,\Delta\mathbf{u}(k) + \\ + \mathbf{K}[\mathbf{y}(k) - \mathbf{C}_e\,\hat{\mathbf{x}}_e(k) + \mathbf{b}(k)]\end{aligned} \tag{19}$$

To calculate the closed-loop transfer function, the initial state is increased, adding the prediction error:

$$\boldsymbol{\varepsilon}(k) = \mathbf{x}_e(k) - \hat{\mathbf{x}}_e(k) \tag{20}$$

Considering only the terms related to $\mathbf{b}(k)$ as they are part of the minimization process, the following state-space system is derived:

$$\begin{bmatrix}\mathbf{x}_e(k+1)\\ \boldsymbol{\varepsilon}(k+1)\end{bmatrix} = \begin{bmatrix}\mathbf{A}_1 & \mathbf{A}_3\\ \mathbf{0} & \mathbf{A}_2\end{bmatrix}\begin{bmatrix}\mathbf{x}_e(k)\\ \boldsymbol{\varepsilon}(k)\end{bmatrix} + \begin{bmatrix}\mathbf{0} & -\mathbf{B}_e\\ -\mathbf{K} & \mathbf{0}\end{bmatrix}\begin{bmatrix}\mathbf{b}(k)\\ \mathbf{u}'(k)\end{bmatrix} \tag{21}$$

$$\mathbf{y}'(k) = \begin{bmatrix}\mathbf{0} & \mathbf{C}_e\end{bmatrix}\begin{bmatrix}\mathbf{x}_e(k)\\ \boldsymbol{\varepsilon}(k)\end{bmatrix} + \begin{bmatrix}\mathbf{I} & \mathbf{0}\end{bmatrix}\begin{bmatrix}\mathbf{b}(k)\\ \mathbf{u}'(k)\end{bmatrix} \tag{22}$$

with $\mathbf{A}_1 = \mathbf{A}_e - \mathbf{B}_e\mathbf{L}$, $\mathbf{A}_2 = \mathbf{A}_e - \mathbf{K}\mathbf{C}_e$, $\mathbf{A}_3 = \mathbf{B}_e\mathbf{L}$.

According to the theory given in Section 3.1, the Youla parameter can be added to robustify the initial controller, since the transfer between $\mathbf{y}'(k)$ and $\mathbf{u}'(k)$ is zero (without measurement noise, the multivariable output $\mathbf{y}'$ depends only on $\boldsymbol{\varepsilon}(k)$, which is independent from $\mathbf{x}_e(k)$ and $\mathbf{u}'(k)$).

4.2 Robustness Under Frequency Constraints

Next step is the definition of the weighting $\mathbf{W}_u$ as a diagonal high-pass filter in state-space formulation:

$$\begin{cases}\mathbf{x}_W(k+1) = \mathbf{A}_W\mathbf{x}_W(k) + \mathbf{B}_W\mathbf{u}(k)\\ \mathbf{z}(k) = \mathbf{C}_W\mathbf{x}_W(k) + \mathbf{D}_W\mathbf{u}(k)\end{cases} \tag{23}$$

Including the $\mathbf{W}_u$ weighting, a new extended state-space description can be emphasized:

$$\begin{bmatrix}\overline{\mathbf{x}}_1(k+1)\\ \boldsymbol{\varepsilon}(k+1)\end{bmatrix} = \begin{bmatrix}\overline{\mathbf{A}}_1 & \overline{\mathbf{A}}_3\\ \mathbf{0} & \mathbf{A}_2\end{bmatrix}\begin{bmatrix}\overline{\mathbf{x}}_1(k)\\ \boldsymbol{\varepsilon}(k)\end{bmatrix} + \begin{bmatrix}\mathbf{0} & -\overline{\mathbf{B}}_{u'}\\ -\mathbf{K} & \mathbf{0}\end{bmatrix}\begin{bmatrix}\mathbf{b}(k)\\ \mathbf{u}'(k)\end{bmatrix} \tag{24}$$

$$\begin{bmatrix}\mathbf{z}(k)\\ \mathbf{y}'(k)\end{bmatrix} = \begin{bmatrix}\overline{\mathbf{C}}_1 & \overline{\mathbf{C}}_2\\ \mathbf{0} & \mathbf{C}_e\end{bmatrix}\begin{bmatrix}\overline{\mathbf{x}}_1(k)\\ \boldsymbol{\varepsilon}(k)\end{bmatrix} + \begin{bmatrix}\mathbf{0} & -\mathbf{D}_W\\ \mathbf{I} & \mathbf{0}\end{bmatrix}\begin{bmatrix}\mathbf{b}(k)\\ \mathbf{u}'(k)\end{bmatrix} \tag{25}$$

with $\overline{\mathbf{x}}_1(k) = \begin{bmatrix}\mathbf{x}^T(k) & \mathbf{u}^T(k-1) & \mathbf{x}_W^T(k)\end{bmatrix}^T$, $\overline{\mathbf{B}}_{u'} = \begin{bmatrix}\mathbf{B}^T & \mathbf{I} & \mathbf{B}_W^T\end{bmatrix}^T$

$$\overline{\mathbf{A}}_1 = \begin{bmatrix}\mathbf{A}-\mathbf{B}\mathbf{L}_1 & \mathbf{B}-\mathbf{B}\mathbf{L}_2 & \mathbf{0}\\ -\mathbf{L}_1 & \mathbf{I}-\mathbf{L}_2 & \mathbf{0}\\ -\mathbf{B}_W\mathbf{L}_1 & \mathbf{B}_W(\mathbf{I}-\mathbf{L}_2) & \mathbf{A}_W\end{bmatrix},\ \overline{\mathbf{A}}_3 = \begin{bmatrix}\mathbf{B}\mathbf{L}\\ \mathbf{L}\\ \mathbf{B}_W\mathbf{L}\end{bmatrix},$$

$$\overline{\mathbf{C}}_1 = \begin{bmatrix}-\mathbf{D}_W\mathbf{L}_1 & \mathbf{D}_W(\mathbf{I}-\mathbf{L}_2) & \mathbf{C}_W\end{bmatrix},\ \overline{\mathbf{C}}_2 = \mathbf{D}_W\mathbf{L}.$$

As described in Section 3.2, a multivariable Youla parameter $\mathbf{Q} \in \Re H_\infty$ is added for robustification purposes leading to a convex optimization problem. Since this problem leads to a $\mathbf{Q}$ parameter which varies in the infinite-dimensional space $\Re H_\infty$, a sub-optimal solution considers for each input/output pairs (i, j) a finite-dimensional subspace generated by an orthonormal base of discrete stable transfer functions such as a polynomial or FIR filter:

$$Q^{ij} = \sum_{l=0}^{n_Q} q_l^{ij} q^{-l} \tag{26}$$

In the state-space formalism, this MIMO Youla parameter can be obtained using a fixed pair $(\mathbf{A}_Q \in \mathbf{R}^{pn_Q \times pn_Q}, \mathbf{B}_Q \in \mathbf{R}^{pn_Q \times p})$ and designing only the variable pair $(\mathbf{C}_Q \in \mathbf{R}^{m \times pn_Q}, \mathbf{D}_Q \in \mathbf{R}^{m \times p})$:

$$\begin{cases}\mathbf{x}_Q(k+1) = \mathbf{A}_Q\mathbf{x}_Q(k) + \mathbf{B}_Q\mathbf{y}'(k)\\ \mathbf{u}'(k) = \mathbf{C}_Q\mathbf{x}_Q(k) + \mathbf{D}_Q\mathbf{y}'(k)\end{cases} \tag{27}$$

with $\mathbf{a}_Q = \begin{bmatrix}\mathbf{0}_{1,n_Q-1} & 0\\ \mathbf{I}_{n_Q-1} & \mathbf{0}_{n_Q-1,1}\end{bmatrix}$, $\mathbf{b}_Q = \begin{bmatrix}1\\ \mathbf{0}_{n_Q-1,1}\end{bmatrix}$, $\mathbf{c}_Q^{ij} = \begin{bmatrix}q_1^{ij}\\ \vdots\\ q_{n_Q}^{ij}\end{bmatrix}$

$$\mathbf{C}_Q = \begin{bmatrix}\mathbf{c}_Q^{11} & \cdots & \mathbf{c}_Q^{1p}\\ \vdots & \ddots & \vdots\\ \mathbf{c}_Q^{m1} & \cdots & \mathbf{c}_Q^{mp}\end{bmatrix},\ \mathbf{D}_Q = \begin{bmatrix}q_0^{11} & \cdots & q_0^{1p}\\ \vdots & \ddots & \vdots\\ q_0^{m1} & \cdots & q_0^{mp}\end{bmatrix},$$

$\mathbf{A}_Q = diag(\mathbf{a}_Q, \cdots, \mathbf{a}_Q)$, $\mathbf{B}_Q = diag(\mathbf{b}_Q, \cdots, \mathbf{b}_Q)$.

Adding this Youla parameter leads to the following closed-loop state-space description:

$$\begin{cases}\mathbf{x}_{cl}(k+1) = \mathbf{A}_{cl}\mathbf{x}_{cl}(k) + \mathbf{B}_{cl}\mathbf{b}(k)\\ \mathbf{z}(k) = \mathbf{C}_{cl}\mathbf{x}_{cl}(k) + \mathbf{D}_{cl}\mathbf{b}(k)\end{cases} \tag{28}$$

with $\mathbf{x}_{cl} = \begin{bmatrix}\overline{\mathbf{x}}_1^T & \boldsymbol{\varepsilon}^T & \mathbf{x}_Q^T\end{bmatrix}^T$,

$$\mathbf{C}_{cl} = \begin{bmatrix} \overline{\mathbf{C}}_1 & \overline{\mathbf{C}}_2 - \mathbf{D}_w \mathbf{D}_Q \mathbf{C}_e & -\mathbf{D}_w \mathbf{C}_Q \end{bmatrix},\ \mathbf{D}_{cl} = -\mathbf{D}_w \mathbf{D}_Q,$$

$$\mathbf{A}_{cl} = \begin{bmatrix} \overline{\mathbf{A}}_1 & \overline{\mathbf{A}}_3 - \overline{\mathbf{B}}_{u'} \mathbf{D}_Q \mathbf{C}_e & -\overline{\mathbf{B}}_{u'} \mathbf{C}_Q \\ \mathbf{0} & \mathbf{A}_2 & \mathbf{0} \\ \mathbf{0} & \mathbf{B}_Q \mathbf{C}_e & \mathbf{A}_Q \end{bmatrix},\ \mathbf{B}_{cl} = \begin{bmatrix} -\overline{\mathbf{B}}_{u'} \mathbf{D}_Q \\ -\mathbf{K} \\ \mathbf{B}_Q \end{bmatrix}.$$

This state-space representation is the crucial point of the robustification method. With the result of the theorem in Section 3, the first step to transform (17) into a LMI consists in multiplying it to the right and to the left with positive definite matrices $\mathbf{\Pi} = \mathrm{diag}(\mathbf{X}_1, \mathbf{I}, \mathbf{I}, \mathbf{I})$ and $\mathbf{\Pi}^{\mathrm{T}}$ as in (Clement and Duc, 2000). This leads to the following inequality:

$$\begin{bmatrix} -\mathbf{X}_1 & \mathbf{X}_1 \mathbf{A}_{cl} & \mathbf{X}_1 \mathbf{B}_{cl} & \mathbf{0} \\ \mathbf{A}_{cl}^{\mathrm{T}} \mathbf{X}_1 & -\mathbf{X}_1 & \mathbf{0} & \mathbf{C}_{cl}^{\mathrm{T}} \\ \mathbf{B}_{cl}^{\mathrm{T}} \mathbf{X}_1 & \mathbf{0} & -\gamma \mathbf{I} & \mathbf{D}_{cl}^{\mathrm{T}} \\ \mathbf{0} & \mathbf{C}_{cl} & \mathbf{D}_{cl} & -\gamma \mathbf{I} \end{bmatrix} < 0 \qquad (29)$$

which is not yet a LMI because terms such as $\mathbf{X}_1 \mathbf{A}_{cl}$ and $\mathbf{X}_1 \mathbf{B}_{cl}$ are not linear in $\mathbf{X}_1$, $\mathbf{C}_Q$ and $\mathbf{D}_Q$. To overcome this problem, the following bijective substitution is introduced (Clement and Duc, 2000):

$$\begin{cases} \mathbf{R}^{n \times n} \to \mathbf{R}^{n \times n} \\ \mathbf{X}_1 = \begin{bmatrix} \mathbf{W}_1 & \mathbf{Z}_1 \\ \mathbf{Z}_1^{\mathrm{T}} & \mathbf{Y}_1 \end{bmatrix} \mapsto \begin{bmatrix} \mathbf{R}_1 & \mathbf{S}_1 \\ \mathbf{S}_1^{\mathrm{T}} & \mathbf{T}_1 \end{bmatrix} = \begin{bmatrix} \mathbf{R}_1 & \mathbf{S}_{11} & \mathbf{S}_{12} \\ \mathbf{S}_{11}^{T} & \mathbf{T}_{11} & \mathbf{T}_{12} \\ \mathbf{S}_{12}^{T} & \mathbf{T}_{12}^{T} & \mathbf{T}_{22} \end{bmatrix} \end{cases} \qquad (30)$$

with $\mathbf{R}_1 = \mathbf{W}_1^{-1}$, $\mathbf{S}_1 = -\mathbf{W}_1^{-1} \mathbf{Z}_1$, $\mathbf{T}_1 = \mathbf{Y}_1 - \mathbf{Z}_1^{\mathrm{T}} \mathbf{W}_1^{-1} \mathbf{Z}_1$.

Next step to the LMI is to multiply (29) on the right with $\mathbf{\Gamma} = \mathrm{diag}\left(\begin{bmatrix} \mathbf{R}_1 & \mathbf{0} \\ \mathbf{S}_1^{\mathrm{T}} & \mathbf{I} \end{bmatrix}, \begin{bmatrix} \mathbf{R}_1 & \mathbf{0} \\ \mathbf{S}_1^{\mathrm{T}} & \mathbf{I} \end{bmatrix}, \mathbf{I}, \mathbf{I} \right)$ and on the left with $\mathbf{\Gamma}^{\mathrm{T}}$. After technical manipulations, the following LMI is obtained:

$$\left[\begin{array}{ccc|ccc|c|c} -\mathbf{R}_1 & \mathbf{0} & \mathbf{0} & \overline{\mathbf{A}}_1 \mathbf{R}_1 & t_1 & t_4 & t_7 & \mathbf{0} \\ * & -\mathbf{T}_{11} & -\mathbf{T}_{12} & \mathbf{0} & t_2 & t_5 & t_8 & \mathbf{0} \\ * & * & -\mathbf{T}_{22} & \mathbf{0} & t_3 & t_6 & t_9 & \mathbf{0} \\ \hline * & * & * & -\mathbf{R}_1 & \mathbf{0} & \mathbf{0} & \mathbf{0} & t_{10} \\ * & * & * & * & -\mathbf{T}_{11} & -\mathbf{T}_{12} & \mathbf{0} & t_{11} \\ * & * & * & * & * & -\mathbf{T}_{22} & \mathbf{0} & t_{12} \\ \hline * & * & * & * & * & * & -\gamma \mathbf{I} & t_{13} \\ \hline * & * & * & * & * & * & * & -\gamma \mathbf{I} \end{array}\right] < 0 \qquad (31)$$

where $t_1 = \overline{\mathbf{A}}_1 \mathbf{S}_{11} - \mathbf{S}_{11} \mathbf{A}_2 - \mathbf{S}_{12} \mathbf{B}_Q \mathbf{C}_e + \overline{\mathbf{A}}_3 - \overline{\mathbf{B}}_{u'} \mathbf{D}_Q \mathbf{C}_e$,

$t_2 = \mathbf{T}_{11} \mathbf{A}_2 + \mathbf{T}_{12} \mathbf{B}_Q \mathbf{C}_e$, $t_3 = \mathbf{T}_{12}^{\mathrm{T}} \mathbf{A}_2 + \mathbf{T}_{22} \mathbf{B}_Q \mathbf{C}_e$,

$t_4 = \overline{\mathbf{A}}_1 \mathbf{S}_{12} - \mathbf{S}_{12} \mathbf{A}_Q - \overline{\mathbf{B}}_{u'} \mathbf{C}_Q$, $t_5 = \mathbf{T}_{12} \mathbf{A}_Q$, $t_6 = \mathbf{T}_{22} \mathbf{A}_Q$,

$t_7 = -\overline{\mathbf{B}}_{u'} \mathbf{D}_Q + \mathbf{S}_{11} \mathbf{K} - \mathbf{S}_{12} \mathbf{B}_Q$, $t_8 = -\mathbf{T}_{11} \mathbf{K} + \mathbf{T}_{12} \mathbf{B}_Q$,

$t_9 = -\mathbf{T}_{12}^{\mathrm{T}} \mathbf{K} + \mathbf{T}_{22} \mathbf{B}_Q$, $t_{10} = \mathbf{R}_1 \overline{\mathbf{C}}_1^{\mathrm{T}}$, $t_{13} = -\mathbf{D}_Q^{\mathrm{T}} \mathbf{D}_w^{\mathrm{T}}$,

$t_{11} = \mathbf{S}_{11}^{\mathrm{T}} \overline{\mathbf{C}}_1^{\mathrm{T}} + \overline{\mathbf{C}}_2^{\mathrm{T}} - \mathbf{C}_e^{T} \mathbf{D}_Q^{T} \mathbf{D}_w^{\mathrm{T}}$, $t_{12} = \mathbf{S}_{12}^{\mathrm{T}} \overline{\mathbf{C}}_1^{\mathrm{T}} - \mathbf{C}_Q^{\mathrm{T}} \mathbf{D}_w^{\mathrm{T}}$.

The whole problem results in the minimization of γ subject to the LMI constraint (31):

$$\min_{LMI} \gamma \qquad (32)$$

5 APPLICATION TO A STIRRED TANK REACTOR

The previous robustification methodology is applied now to the simplified MIMO model of a stirred tank reactor presented in the transfer function formalism in (Camacho and Bordons, 2004):

$$\begin{bmatrix} Y_1(s) \\ Y_2(s) \end{bmatrix} = \begin{bmatrix} 1/(1+0.7s) & 5/(1+0.3s) \\ 1/(1+0.5s) & 2/(1+0.4s) \end{bmatrix} \begin{bmatrix} U_1(s) \\ U_2(s) \end{bmatrix} \qquad (33)$$

where Y_1 and Y_2 are the effluent concentration and the reactor temperature, U_1 and U_2 are the feed flow rate and the coolant flow, respectively.

Starting from the state-space representation of this 2 inputs/ 2 outputs model discretized for a sampling time $T_e = 0.03$ min, an integral action is added leading to an extended state-space model. For simplicity reasons of multivariable MPC, the same prediction horizons $N_1 = 1$, $N_2 = 3$ and $N_u = 2$ were used for all outputs and control signals, and the same weights as in (Camacho and Bordons, 2004) $\widetilde{R}_J = 0.05 \mathbf{I}_{N_u}$ and $\widetilde{Q}_J = \mathbf{I}_{N_2 - N_1 + 1}$.

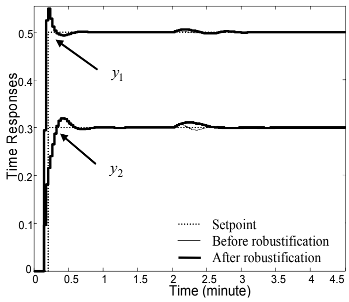

Figure 5: y_1 and y_2 before and after robustification.

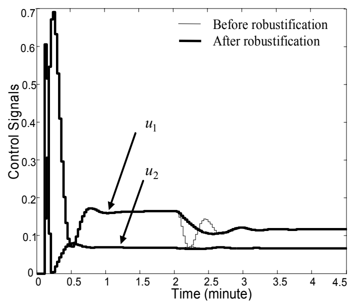

Figure 6: u_1 and u_2 before and after robustification.

Figures 5 shows the time responses obtained for a step reference of 0.5 for y_1, and 0.3 for y_2, and the disturbance rejection for a step disturbance of 0.05 applied to u_1 at $t = 2$ min. Figure 6 shows the control signals u_1 and u_2.

For robustness under additive uncertainties at high frequency, a high-pass filter is used for each control signal, as described in Section 4.2 which transfer form is $\mathbf{W_u} = \mathbf{I}_2 (1 - 0.7q^{-1}) / 0.3$. Using the optimization procedure based on LMIs gives a multivariable Youla parameter as a 2×2 matrix of polynomials of order $n_Q = 20$.

Figure 7 shows the singular values analysis of transfer from **b** to control signals **u** (from Figure 4). The greatest value of maximal singular values represents the H_∞ norm. We can remark that this H_∞ norm has been reduced. In this way the stability robustness is improved with respect to high-frequency additive unstructured uncertainties.

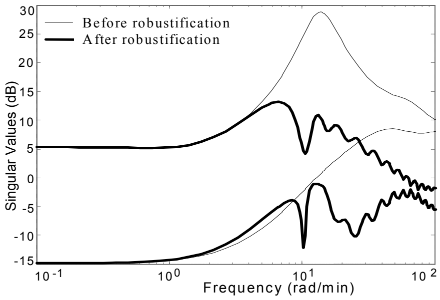

Figure 7: Singular values before and after robustification.

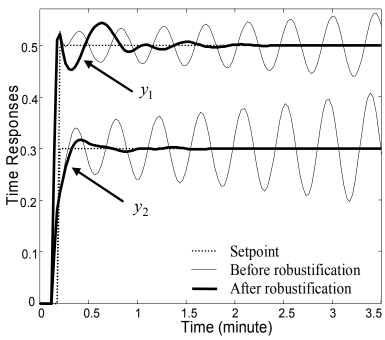

Figure 8: y_1 and y_2 before and after robustification.

Figures 5 and 6 show that after robustification the input/output behaviour is unchanged, but the disturbance is rejected more slowly by the robustified controller. In fact, the robustified controller has a slower disturbance rejection, but a higher robust stability. To support this, a high frequency neglected dynamics of the actuator u_1 has been considered. Thus the transfer between y_1 / u_1 corresponds to $1/(1+0.7s)(1+0.07s)$. Figure 8 illustrates that the initial controller behaviour is destabilized by this uncertainty, but the robustified controller remains stable; it also shows the influence of the considered unstructured uncertainty to y_2.

6 CONCLUSIONS

This paper has presented a new MIMO complete methodology which enables robustifing an initial multivariable MPC controller in state-space formalism using the Youla parameter framework. In order to improve robustness towards unstructured uncertainties, a H_∞ convex optimization problem was solved using the LMIs techniques. The major advantage of the developed structure is the state-space formulation of this MPC robustification problem for MIMO systems with a reduced computational effort compared to the transfer function formalism. This method can also be applied to non square systems, which otherwise are more difficult to control. This technique enables also the use of time-domain templates to manage the compromise between stability robustness and nominal performance.

REFERENCES

Boyd, S., Barratt, C., 1991. *Linear controller design. Limits of performance*, Prentice Hall.

Boyd, S., Ghaoui, L.El., Feron, E., Balakrishnan, V., 1994. *Linear matrix inequalities in system and control theory*, SIAM Publications, Philadelphia.

Camacho, E.F., Bordons, C., 2004. *Model predictive control,* Springer-Verlag. London, 2nd edition.

Clement, B., Duc, G., 2000. A multiobjective control via Youla parameterization and LMI optimization: application to a flexible arm, IFAC Symposium on Robust Control and Design, Prague.

Dumur, D., Boucher, P., 1998. *A Review introduction to linear GPC and applications*, Journal A, 39(4), pp. 21-35.

Kouvaritakis, B., Rossiter, J.A., Chang, A.O.T., 1992. *Stable generalized predictive control: an algorithm with guaranteed stability*, IEE Proceedings-D, 139(4), pp. 349-362.

Maciejowski, J.M., 1989. *Multivariable feedback design*, Addison-Wesley Publishing Company, Wokingham, England.

Maciejowski, J.M., 2001. *Predictive control with constrains*, Prentice Hall.

Magni, J.F., 2002. *Robust modal control with a toolbox for use with MATLAB*, Springer.

Yoon, T.W., Clarke, D.W. 1995. *Observer design in receding-horizon predictive control*, International Journal of Control, 61(1), pp. 171-191.